Dipole moment functions of the hydrogen halides

J. F. OgilvieW. R. RodwellR. H. Tipping

Citation: The Journal of Chemical Physics **73**, 5221 (1980); doi: 10.1063/1.439950
View online: http://dx.doi.org/10.1063/1.439950
View Table of Contents: http://aip.scitation.org/toc/jcp/73/10
Published by the American Institute of Physics

Dipole moment functions of the hydrogen halides

J. F. Ogilvie[a)]

Department of Chemistry, University of Kuwait, P.O. Box 5969, Kuwait

W. R. Rodwell

Research School of Chemistry, Australian National University, P.O. Box 4, Canberra A.C.T. 2600, Australia

R. H. Tipping

Department of Physics, University of Nebraska at Omaha, Omaha, Nebraska 68182
(Received 23 June 1980; accepted 4 August 1980)

Experimental intensity data for vibration–rotational transitions and molecular beam data of the hydrogen halide diatomic molecules (HF, HCl, HBr, and HI) have been analyzed, and the coefficients of a power series expansion of the dipole moment functions valid near the equilibrium internuclear separations have been determined. *Ab initio* quantum chemical computations of the dipole moments have also been carried out over a wide range of internuclear separations for HF, HCl, and HBr, and the factors affecting the accuracy of these results have been critically examined. The long-range values from these computations have been combined with the results near equilibrium in the form of a Padé approximant that embodies the correct asymptotic behavior.

I. INTRODUCTION

In a previous review[1] of the influence of the potential function on vibration–rotational wave functions and matrix elements, the results were applied to a detailed analysis of the spectral intensities of the diatomic hydrogen halide molecules. The dipole moment function was represented by a power series expansion in terms of the reduced displacement from the equilibrium internuclear separation $x=(R-R_e)/R_e$ and the number of coefficients in each series which could be determined was limited by the availability of experimental intensity data for the higher overtones. With this assumed form, the pure rotational and vibration–rotational dipole transition moments can be calculated from the corresponding matrix elements of powers of x. Analytic approximations to these matrix elements derived using the hypervirial theorem and quantum mechanical sum rules[2,3] were published for the 0–0 through the 0–4 bands.[1] Since the appearance of this article, this method has been extended to greater accuracy and higher overtones.[4] During the same period extensive progress has been made on the calculation of matrix elements via higher order perturbation methods.[5]

Paralleling these theoretical advances, in the past few years extensive experimental intensity data for HCl,[6] HBr,[7] and HI[8] have been reported, so that at present a comprehensive set of accurate intensity data from the pure rotational band through the 0–5 band is now available for all of the stable hydrogen halides. These data enable one to obtain the first six terms of the near equilibrium series expansion of the dipole moment function; this analysis is presented in the following section.

It is well known, however, that the power series representation is of limited use in predicting higher overtone intensities (necessary, for example, for a quantitative treatment of chemical dynamics experiments and laser spectra[9]). This is due primarily to the divergence of the series for large displacements. In order to circumvent this problem, recourse has been made to *ab initio* computations of dipole moment functions. The accuracy of these calculations has improved markedly in the last few years, and dipole moment functions for a number of diatomic molecules over a large range of internuclear separations have been reported.[10] In Sec. III we present new results of *ab initio* computations for HF, HCl, and HBr. These results agree reasonably well (in shape and absolute magnitude) with the experimentally determined series near equilibrium and, in addition, exhibit the correct long-range asymptotic dependence on internuclear separation (i.e., R^{-4}). For HI we use existing computations of the dipole moment.[11]

In order to utilize the high accuracy of the experimental data and at the same time incorporate the correct asymptotic dependence of the theoretical calculations, we introduce in Sec. IV a semiempirical model for the dipole moment function in the form of a Padé approximant. We discuss the simplest form which reduces to the correct united and separated atom limits, which has the correct long- and short-range dependence on R, and which is sufficiently flexible to reproduce the conventional power series near equilibrium. Numerical parameters for this dipole moment function are presented for all the hydrogen halides and, in the final section, we compare the present results with previous work, and discuss the merits of the Padé form for extrapolation in order to estimate higher overtone intensities.

II. BEHAVIOR NEAR EQUILIBRIUM SEPARATION

For the stable hydrogen halide molecules, accurate spectroscopic information is available from molecular beam studies and from absorption measurements in the pure rotational, fundamental, and first four overtone vibration–rotational bands. We shall first analyze the available intensity data in the conventional way,[1] i.e., by assuming a power series representation for the di-

[a)]Current address (1980): Research School of Chemistry, Australian National University.

 0021-9606/80/225221-09$01.00

TABLE I. Experimental rotationless dipole moment matrix elements (D).

	HF	$H^{35}Cl$	$H^{79}Br$	HI
$M_0^0(0)$[a]	1.826526[b]	1.10847[g]	0.82656[k]	0.4477[n]
$M_0^1(0)$ (10^{-2})	9.850[c]	7.12[h]	3.7036[l]	−0.4016[o]
$M_0^2(0)$ (10^{-3})	−12.53[d]	−7.75[h]	−2.73[m]	1.796[p]
$M_0^3(0)$ (10^{-3})	1.628[e]	0.515[i]	−0.3543[m]	−1.120[p]
$M_0^4(0)$ (10^{-4})	−3.48[f]	−0.365[j]	2.194[m]	3.954[q]
$M_0^5(0)$ (10^{-5})	8.79[f]	−1.01[j]	−7.6[m]	−13.6[q]

[a]The quantity actually measured was $|\langle 0J|M|0J\rangle|$; this has been corrected by terms of order γ^2 to yield $|\langle 0|M|0\rangle|$ which, by convention, we will regard as positive.
[b]Reference 12.
[c]Reference 13.
[d]Reference 14.
[e]Reference 15.
[f]Reference 16.
[g]Reference 17.
[h]Reference 18.
[i]Reference 19.
[j]Reference 6.
[k]Reference 20.
[l]Reference 21.
[m]Reference 7.
[n]Reference 22.
[o]Reference 23.
[p]Reference 24.
[q]Reference 8.

pole moment function in terms of the reduced displacement from equilibrium

$$\mu(x)=\sum_{i=0}^{5} M_i x^i \ . \tag{1}$$

The intensity of a vibration–rotational band ($v=n\leftarrow v=0$) in absorption depends on the square of the rotationless dipole moment matrix element $M_0^n(0)$ which, using Eq. (1), we can write

$$M_0^n(0)\equiv\langle n0|\mu(x)|00\rangle \equiv\langle n|\mu|0\rangle=\sum_{i=0}^{5} M_i\langle n|x^i|0\rangle \ . \tag{2}$$

Experimental values for the $M_0^n(0)$ for n up to 5 are collected in Table I.

As discussed previously,[1] accurate analytic approximations to the matrix elements of x^i have been given for the Dunham potential

$$V(x)=\gamma^{-2}B_e x^2\left(1+\sum_{i=1}^{6} a_i x^i\right) \tag{3}$$

TABLE II. Dunham potential coefficients.

	HF[a]	$H^{35}Cl$[b]	$H^{79}Br$[c]	HI[d]
a_1	−2.2538	−2.36323	−2.43659	−2.54625
a_2	3.4882	3.66127	3.845638	4.05336
a_3	−4.4986	−4.76387	−5.07504	−5.4421
a_4	4.704	5.54872	5.4406	6.6407
a_5	−2.91	−5.80853	−3.07336	−6.9146
a_6	−1.76	4.42395	−2.376	0.38
γ (10^{-3})	10.126735	7.0836104	6.390289	5.640243

[a]Reference 25.
[b]Reference 26.
[c]Reference 27.
[d]Reference 28.

TABLE III. Coefficients of the dipole moment[a] power series expansion.

	HF	$H^{35}Cl$	$H^{79}Br$	HI
M_0	1.80306	1.09333	0.81788	0.44722
M_1	1.39366	1.20597	0.65545	−0.07404
M_2	−0.0583	0.0399	0.3516	0.5057
M_3	−0.8861	−1.6349	−1.6974	−1.9794
M_4	−0.599	−0.700	−0.687	−0.053
M_5	−0.931	5.011	1.963	−0.0015

[a]Units are D; 1 D = 3.33564×10^{-30} C m.

as expansions in powers of γ, the coefficients of which are functions of the potential parameters a_i. The numerical values used in the present study are listed in Table II. Because the measured intensities are proportional to the squares of the corresponding matrix elements, there is ambiguity in determining the relative signs of the transition moments. This condition in general leads to 2^n sets of independent coefficients M_i [Eq. (1)] which satisfy the experimental $|M_0^n(0)|$. The uncertainty can however be eliminated by including the effects of vibration–rotation interaction if individual line strengths are known. The line strengths are proportional to the squares of vibration–rotational matrix elements which can be written

$$\langle v'J'|\mu(x)|vJ\rangle^2=\langle v'0|\mu(x)|v0\rangle^2 F_v^{v'}(m) =\langle v+n0|\mu(x)|v0\rangle^2[1+C_n(v)m+D_n(v)m^2+\cdots] \ , \tag{4}$$

where $F_v^{v'}(m)$ is the Herman–Wallis factor, and m is a running index equal to $J+1$ for R lines and $-J$ for P lines. Analytic expressions for $C_n(v)$ and $D_n(v)$ have been published previously for $n=0$ to 4[29]; the leading terms for $C_5(0)$ and $D_5(0)$ needed in the present study are given in the Appendix. More accurate expressions and results for higher overtones will be published[30] in a separate article analyzing the higher overtone intensity data of HCl.[6] The important point to note is that these coefficients depend linearly on M_i (and on the potential parameters), and the comparison between theory and experiment not only leads to a unique set of signs (within the limits of experimental error) but also tests the internal consistency of the intensity data. With the choice of signs given in Table I, the coefficients M_i that give the best overall fit are listed in Table III. The comparison between theoretical and experimental C and D coefficients is presented in Table IV. As can be seen from the table, with few exceptions the overall agreement is very satisfactory.

The dipole moment functions thus obtained as truncated series expansions are valid within a small range of internuclear separations delimited by the extent of the input intensity data. In the present case in which the highest overtone used is the fourth, this range is approximately $-0.2<x<0.4$. Outside this range, the series diverge rapidly as can be seen from the third columns of Tables V through VIII, where we have tabulated these series expansions for various values of x. Because higher vibrational wave functions have significant amplitude at increasingly larger internuclear separations where these series begin to diverge, their use in esti-

TABLE IV. Experimental and theoretical Herman–Wallis coefficients.

	HF		$H^{35}Cl$		$H^{79}Br$		HI	
Coefficient	Experimental	Theoretical	Experimental	Theoretical	Experimental	Theoretical	Experimental	Theoretical
$C_1(0)$	-4.96×10^{-2} [a]	-5.38×10^{-2}	-2.60×10^{-2} [e]	-2.66×10^{-2}	-3.12×10^{-2} [h]	-3.25×10^{-2}	1.22×10^{-1} [j]	1.38×10^{-1}
$D_1(0)$	1.3×10^{-3} [a]	8.6×10^{-4}	4.5×10^{-4} [e]	2.7×10^{-4}	1.3×10^{-3} [h]	4.3×10^{-4}	6.7×10^{-4} [j]	3.8×10^{-3}
$C_2(0)$	-1.93×10^{-2} [b]	-2.39×10^{-2}	-8.60×10^{-3} [e]	-5.75×10^{-3}	-2.53×10^{-2} [i]	-1.78×10^{-2}	2.54×10^{-2} [k]	3.22×10^{-2}
$D_2(0)$	-2.8×10^{-4} [b]	2.7×10^{-4}	4.1×10^{-4} [e]	3.7×10^{-4}	2.2×10^{-4} [i]	1.1×10^{-3}	1.5×10^{-3} [k]	-3.6×10^{-4}
$C_3(0)$	-2.18×10^{-2} [c]	-1.72×10^{-2}	1.70×10^{-2} [f]	8.54×10^{-3}	1.87×10^{-2} [i]	1.72×10^{-2}	1.58×10^{-2} [k]	1.23×10^{-2}
$D_3(0)$	1.4×10^{-3} [c]	-8.7×10^{-5}	···	8.7×10^{-4}	···	-1.6×10^{-4}	1.12×10^{-4} [l]	-1.4×10^{-5}
$C_4(0)$	< 0 [d]	-3.21×10^{-3}	8.49×10^{-2} [g]	4.96×10^{-2}	1.25×10^{-2} [d]	1.25×10^{-2}	1.76×10^{-2} [l]	1.31×10^{-2}
$D_4(0)$	···	1.3×10^{-4}	1.2×10^{-2} [g]	-3.5×10^{-3}	···	3.9×10^{-4}	2.1×10^{-3} [l]	1.6×10^{-4}
$C_5(0)$	< 0 [d]	-4.01×10^{-2}	7.65×10^{-2} [g]	7.72×10^{-2}	···	2.61×10^{-2}	1.73×10^{-2} [l]	1.85×10^{-2}
$D_5(0)$	···	6.2×10^{-4}	9.6×10^{-3} [g]	9.5×10^{-3}	···	6.9×10^{-4}	1.5×10^{-3} [l]	2.9×10^{-4}

[a] Reference 13. [d] Reference 16. [g] Reference 6. [j] Reference 23.
[b] Reference 14. [e] Reference 18. [h] Reference 21. [k] Reference 24.
[c] Reference 15. [f] Reference 19. [i] Reference 7. [l] Reference 8.

mating higher overtone intensities is subject to considerable error. We discuss a more reasonable representation suitable for extrapolation in the following sections.

III. BEHAVIOR AT LARGER SEPARATIONS

Although intensity measurements provide information about the dipole moment function near equilibrium separation, no experimental data of comparable accuracy are available for use outside this region. However, the range of larger separations, up to $x \sim 6$, is especially important because this range of vibrational amplitudes is accessible to molecules in vibrational states approaching the dissociation limit. In order to have a dipole moment function with some validity for these states, we must at present have recourse to purely theoretical data from *ab initio* quantum computations. For this reason we have undertaken new calculations for HF, HCl, and HBr, whereas some results already exist[11] for the 54-electron molecule HI.

To ensure the correct dissociation behavior of HF, HCl, and HBr in their $^1\Sigma^+$ ground electronic states to the separated atom limits of neutral H ^2S and halogen ^2P, we

TABLE V. Dipole moment (D) and energy (aJ) of HF as a function of internuclear separation.

R (10^{-10} m)	x	μ_{series}	$\mu_{\text{Padé}}$	μ_{MCSCF}	E_{MCSCF} [a,b]
0.6	−0.346	1.347	1.283	1.362	0.14667
0.7	−0.236	1.481	1.476	1.505	0.95187
0.8	−0.127	1.626	1.626	1.653	1.27561
0.9	−0.018	1.778	1.777	1.793	1.36473
0.917	0.0002	1.803	1.803	1.816	1.36637
0.93	0.014	1.823	1.823	1.832	1.36573
1.0	0.091	1.928	1.928	1.913	1.34026
1.1	0.200	2.071	2.070	1.999	1.26369
1.2	0.309	2.194	2.182	2.037	1.16716
1.3	0.418	2.281	2.223	2.017	1.06772
1.4	0.527	2.308	2.132	1.935	0.97431
1.5	0.636	2.243	1.877	1.794	0.89139
1.6	0.745	2.044	1.508	1.609	0.82077
1.7	0.854	1.656	1.126	1.397	0.76260
1.9	1.072	0.025	0.571	0.970	0.67971
2.1	1.291	−3.4	0.292	0.619	0.63111
2.4	1.618	−14.3	0.121	0.290	0.59628
2.7	1.945	−36.7	0.058	0.132	0.58329
3.1	2.381	−98.	0.026	0.047	0.57794
3.5	2.818		0.014	0.019	0.57664
3.9	3.254		0.0078	0.0092	0.57633
4.4	3.799		0.0044	0.0046	0.57624
5.0	4.454		0.0024	0.0025	0.57623
6.0	5.545		0.0011	0.0011	0.57622
7.0	6.635		0.00055	0.00055	0.57622
8.5	8.271		0.00025	0.00025	0.57622
10.0	9.908		0.00013	0.00013	0.57622
13.0	13.180		0.000045	0.000046	0.57622
16.0	16.452		0.000020	0.000020	0.57622

[a] $E^{\text{Total}}_{\text{MCSCF}} = -E_{\text{MCSCF}} - 435.0$.
[b] Conversion factor: 1 atomic unit = 4.359816 aJ in Tables V–VII.

TABLE VI. Dipole moment (D) and energy (aJ) of HCl as a function of internuclear separation.

R (10^{-10} m)	x	μ_{series}	$\mu_{Padé}$	μ_{MCSCF}	E_{MCSCF} [a]
0.90	−0.294	0.767	0.752	0.867	0.18489
1.0	−0.215	0.848	0.846	0.937	0.65783
1.1	−0.137	0.933	0.933	1.012	0.89914
1.2	−0.058	1.023	1.023	1.089	1.00255
1.25	−0.019	1.070	1.070	1.127	1.02117
1.275	0.0004	1.094	1.094	1.146	1.02450
1.3	0.020	1.117	1.117	1.164	1.02453
1.35	0.059	1.165	1.165	1.198	1.01638
1.4	0.098	1.211	1.211	1.229	0.99969
1.5	0.176	1.299	1.299	1.280	0.94960
1.6	0.255	1.379	1.375	1.312	0.88765
1.7	0.334	1.452	1.434	1.320	0.82202
1.8	0.412	1.522	1.463	1.301	0.75758
2.0	0.569	1.717	1.382	1.181	0.64273
2.2	0.726	2.181	1.092	0.968	0.55407
2.4	0.883	3.328	0.729	0.718	0.49230
2.7	1.118	7.8	0.347	0.396	0.43950
3.0	1.354	19.2	0.168	0.199	0.41606
3.4	1.668	54.8	0.072	0.077	0.40493
3.9	2.060		0.030	0.027	0.40149
4.4	2.452		0.015	0.012	0.40083
5.0	2.923		0.0076	0.0062	0.40068
6.0	3.708		0.0030	0.0028	0.40065
7.0	4.492		0.0015	0.0014	0.40065
8.5	5.669		0.00063	0.00063	0.40065
10.0	6.846		0.00032	0.00033	0.40065
13.0	9.200		0.00011	0.00011	0.40065
16.0	11.554		0.00005	0.00005	0.40065

[a] $E^{Total}_{MCSCF} = -E_{MCSCF} - 2005.0$.

describe the electronic structures of the molecules by two-term multiconfiguration self-consistent field (MCSCF) wave functions. The pairs of configurations were $1\sigma^2 2\sigma^2 3\sigma^2 1\pi^4$ and $1\sigma^2 2\sigma^2 4\sigma^2 1\pi^4$ for HF, ... $4\sigma^2 5\sigma^2 2\pi^4$ and .... $4\sigma^2 6\sigma^2 2\pi^4$ for HCl, and .... $1\delta^4 7\sigma^2 8\sigma^2 4\pi^4$ and .... $1\delta^4 7\sigma^2 9\sigma^2 4\pi^4$ for HBr; in each case the functions deleted and added between the pair of configurations are essentially the bonding and antibonding σ orbitals, respectively. Such wave functions have in previous work been shown for HF [31] and HI [11] to reproduce satisfactorily the experimental dipole moment functions for these molecules. The HF results presented here differ from the previous ones, [31] in fact, in only some basis set details, but our new computations were necessary in order to extend the range of internuclear separations to meet our present requirements.

TABLE VII. Dipole moment (D) and energy (aJ) of HBr as a function of internuclear separation.

R (10^{-10} m)	x	μ_{series}	$\mu_{Padé}$	μ_{MCSCF}	E_{MCSCF} [a]
1.1	−0.222	0.705	0.703	0.844	0.34899
1.2	−0.152	0.732	0.732	0.869	0.59058
1.3	−0.081	0.768	0.768	0.900	0.70798
1.4	−0.010	0.811	0.811	0.933	0.74878
1.414	−0.0003	0.818	0.818	0.937	0.75026
1.42	0.004	0.820	0.820	0.939	0.75063
1.44	0.018	0.830	0.830	0.945	0.75083
1.5	0.061	0.858	0.858	0.963	0.74313
1.6	0.131	0.906	0.906	0.988	0.71031
1.7	0.202	0.950	0.950	1.004	0.66277
1.8	0.273	0.987	0.984	1.007	0.60859
1.9	0.343	1.015	1.005	0.993	0.55298
2.0	0.414	1.033	1.004	0.961	0.49926
2.2	0.555	1.038	0.920	0.845	0.40482
2.4	0.697	1.031	0.734	0.676	0.33266
2.6	0.838	1.087	0.520	0.494	0.28252
2.9	1.050	1.600	0.278	0.270	0.23939
3.2	1.262	3.338	0.147	0.134	0.21986
3.6	1.545	9.78	0.069	0.052	0.21030
4.0	1.828	25.2	0.036	0.023	0.20754
4.5	2.182	67.7	0.018	0.011	0.20666
5.0	2.535		0.010	0.0070	0.20645
6.0	3.242		0.0039	0.0035	0.20638
7.0	3.949		0.0019	0.0018	0.20637
8.5	5.010		0.00080	0.00080	0.20637
10.0	6.070		0.00040	0.00041	0.20637
13.0	8.191		0.00014	0.00014	0.20637
16.0	10.312		0.00006	0.00006	0.20637

[a] $E^{Total}_{MCSCF} = -E_{MCSCF} - 11217.0$

TABLE VIII. Dipole moment (D) of HI as a function of internuclear separation.

R (10^{-10} m)	x	μ_{series}	$\mu_{Padé}$	μ_{MCSCF} [a]
0.9525	−0.408	0.695	0.465	0.823
1.0584	−0.342	0.610	0.548	0.789
1.1642	−0.276	0.548	0.536	0.747
1.2171	−0.244	0.524	0.519	0.732
1.2700	−0.211	0.504	0.502	0.723
1.3229	−0.178	0.487	0.487	0.712
1.3494	−0.161	0.481	0.480	0.707
1.4288	−0.112	0.464	0.465	0.694
1.4817	−0.079	0.457	0.457	0.687
1.5875	−0.013	0.448	0.448	0.674
1.6404	0.020	0.446	0.446	0.668
1.6934	0.052	0.444	0.444	0.661
1.7992	0.118	0.442	0.442	0.645
1.9580	0.217	0.435	0.435	0.614
2.1167	0.316	0.412	0.413	0.571
2.2755	0.414	0.361	0.373	0.515
2.4871	0.546	0.231	0.298	0.424
2.7782	0.727	−0.113	0.194	0.290
3.1751	0.973	−1.017	0.102	0.148
3.7042	1.302	−3.308	0.046	0.061
4.2334	1.631	−7.27	0.024	0.032
4.7626	1.960	−13.4	0.014	0.020
5.2918	2.289	−22.2	0.0085	0.013
10.5835	5.578		0.0007	0.0007
13.2294	7.222		0.0004	0.0004

[a] Reference 11.

The molecular orbitals were expanded in terms of basis sets of Gaussian-type functions. The atomic sets were based on the fluorine 11s6p set of van Duijneveldt, [32] the hydrogen 6s and chlorine 12s9p sets of Huzinaga, [33,34] and the bromine 14s11p5d set of Dunning. [35,36] To ensure that the bases had sufficient flexibility in the valence region, we extended the halogen basis sets at the diffuse end by adding an s and a set of p functions ($\zeta_{sF} = 0.09$, $\zeta_{sCl} = 0.08$, $\zeta_{sBr} = 0.06$, $\zeta_{pF} = 0.07$, $\zeta_{pCl} = \zeta_{pBr} = 0.05$) according to previous practice. [37,38] These primitive atomic basis sets were further augmented by two p polarization function sets on hydrogen ($\zeta_{pH} = 1.0, 0.25$), two d polarization function sets each on fluorine ($\zeta_{dF} = 1.50, 0.35$) and chlorine ($\zeta_{dCl} = 1.0, 0.25$), and a single d function set on bromine ($\zeta_{dBr} = 0.35$). The exponents of the H, F, and Cl polarization functions were based on published values, [32,37–39] supported by our own studies, while that for the Br d polarization function was optimized. We expect the finding [11] for HI, that f functions, included to polarize occupied d orbitals, are unimportant in determining the dipole moment, to hold also for HBr. The resulting primitive basis sets were contracted as follows:

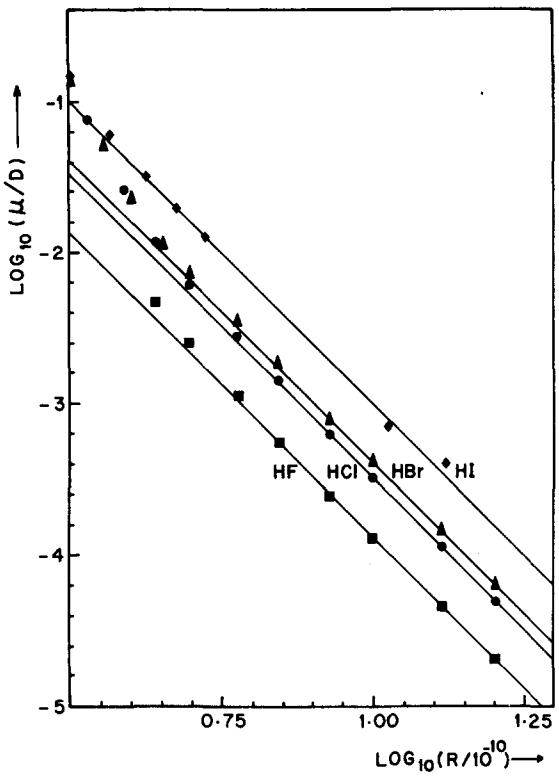

FIG. 1. Log–log plot of MCSCF dipole moment functions vs internuclear separation for the hydrogen halides in the long-range region: ■, HF; ●, HCl; ▲, HBr; ◆, HI. The solid lines have been drawn with slopes equal to −4.

$$\text{HF}:(12s7p2d/6s2p)\rightarrow[7s5p2d/4s2p]\,,$$

$$\text{HCl}:(13s10p2d/6s2p)\rightarrow[9s7p2d/4s2p]\,,$$

$$\text{HBr}:(15s12p6d/6s2p)\rightarrow[11s9p4d/4s2p]\,,$$

by grouping into single functions only the appropriate numbers of innermost orbitals on each atom. Such a contraction scheme preserves the full flexibility of the primitive basis set in the valence region and avoids the well known difficulty for third-row atoms, in this case bromine, of finding efficient segmented contraction schemes.[35] All the computations were performed by means of an established MCSCF program.[40]

The computed total energies and dipole moments are listed in Tables V–VII. Agreement between experimental (M_0 in Table III) and computed (1.8156 D at 91.7 pm for HF; 1.1455 D at 127.5 pm for HCl, and 0.9369 D at 141.4 pm for HBr) equilibrium dipole moments provides a basis for confidence that the computed values for separations beyond the region of applicability of the experimentally derived polynomial functions may exhibit similar accuracy. A further check on the computed results in the long-range region, most pertinent to our problem, is that the dipole moment should decay asymptotically[41] as R^{-4}. This dependence is due to an inductive effect that should be reflected in our MCSCF wave functions; indeed, the log–log plot of computed value of dipole moment against internuclear separation in Fig. 1 demonstrates an essentially exact R^{-4} dependence for $R > 0.85$ nm for HF, HCl, and HBr. In examining this long-range behavior, we note that it is necessary to continue the SCF iterations to a more stringent convergence criterion than is required for energy convergence in order to ensure that the dipole moments have sufficient numerical precision; perhaps for this reason the HI results[11] at 1.0584 and 1.3229 nm do not conform to the expected behavior as demonstrated in Fig. 1.

For $R \gtrsim \sim 0.85$ nm we can therefore expect the MCSCF curves to be at least parallel to the true curves. We can also make some observations about the expected accuracy of the MCSCF curve in that region because there the dipole moment essentially depends linearly upon the quadrupole moment of the halogen atom and the polarizability of atomic hydrogen. Error in the computed halogen quadrupole results from basis set deficiencies, neglect of electron correlation, and the fact that our MCSCF wave function will have a dissociation limit with not strictly full ^2P symmetry for the halogen. We can estimate the magnitude of the latter effect, which is just the usual loss of radial equivalence between singly and doubly occupied p-atomic orbitals in restricted Hartree–Fock computations that lack the imposition of spherical symmetry, by comparing the halogen quadrupole obtained from an SCF computation with p-orbital equivalence imposed and that obtained without this restriction. With our basis choice we find that, for fluorine, imposition of symmetry equivalence decreases the quadrupole moment by ~12%. We would expect electron correlation to contract the fluorine electron density, thereby decreasing the quadrupole, perhaps by a further 10%–20%. Our basis set should be sufficiently flexible to yield an SCF quadrupole moment near the limiting Hartree–Fock value. Because no electron correlation is involved in computations for the hydrogen atom, any deficiencies in the ability of our wave functions to represent the polarization of the H atom must result from inadequacies of the basis set. Previous work[42] indicates that our hydrogen basis is adequate for computations of polarizabilities of hydrogen-containing molecules; however, for an isolated H atom some deficiencies may be present. Thus, for HF at $R = 1.0$ nm and our previous fluorine basis set, we find that improving the hydrogen basis set (up to ten s and four sets of p functions) increases the dipole moment to what appears to be a limiting value of ~0.00019 D, an increase of about half. The main deficiency in the basis set for the description of hydrogen polarizability is probably in the p-function set. Fortunately, the adjustments required to our HF long-range dipole moments, to correct for errors in the fluorine quadrupole and in the hydrogen polarizability, are of opposite signs and largely cancel; as a result, we expect the computed long range dipole moments to underestimate the true values, but by not more than ~20%.

The values of R_e interpolated from these MCSCF computations (91.8 pm for HF, 128.8 pm for HCl, and 143.3 pm for HBr) agree satisfactorily with experiment[25] (91.68, 127.45, and 141.4 pm, respectively). The corresponding energy depths of the potential wells are 0.790 aJ for HF, 0.624 aJ for HCl, and 0.545 aJ for HBr, compared with values[25] of 0.987, 0.746, and 0.638 aJ, respectively, from experiment.

TABLE IX. Coefficients of the dipole magnent function in Padé approximant form.

	HF	$H^{35}Cl$	$H^{79}Br$	HI
M_0 (D)	1.80306	1.09333	0.81788	0.44722
e_1	2.227	1.897	2.199	3.166
e_2	1.311	0.871	0.808	2.393
e_3	0.550	1.465	1.483	2.243
e_4	1.044	1.829	3.868	11.794
e_5	1.112	−4.137	−2.612	10.380
e_6	12.095	13.886	13.209	7.423
e_7	0.722	0.416	0.255	−0.653

IV. REPRESENTATION BY RATIONAL FUNCTIONS

The representation of data by finite polynomials has serious practical and theoretical limitations.[43] Rational functions (ratios of finite polynomials) can provide an accurate alternative representation of the required data without such limitations. In the present case, for each hydrogen halide we have determined six coefficients in the series expansion of the dipole moment function. Furthermore, we know from theoretical considerations[41] that the dipole moment function should approach zero in the united atom limit as R^3, and again approach zero in the separated atom limit as R^{-4}; at equilibrium ($R=R_e$ or $x=0$) it must equal M_0. Unlike the cases of CO[44] or NO[45] for which the dipole moment function has two extrema, our *ab initio* results suggest that the corresponding functions for the hydrogen halides do not go through zero at finite R. All these criteria can be met by a functional dependence of the form

$$\mu(x)=\frac{M_0(1+x)^3}{1+\sum_{i=1}^{5} e_i x^i + e_7 x^7}\,. \tag{5}$$

If the coefficients e_i, $1\le i\le 5$, are determined so as to yield an exact fit to the derivatives of the series expansion at $x=0$, then the rational function constitutes a Padé approximant. In practice we can determine the coefficient e_7 by fitting one value of $\mu(x)$ for a value of R in the long-range region to the *ab initio* results. However, because of the distinction between R^{-4} and x^{-4} at finite R, we have found that a better fit can be obtained by the Padé approximant in the form

$$M(x)=\frac{M_0(1+x)^3}{1+\sum_{i=1}^{7} e_i x^i}\,, \tag{6}$$

where two coefficients e_6 and e_7 are fitted to the long-range *ab initio* results. For HF, HCl, and HBr, we have used the values of $\mu(x)$ at 0.85 and 1.6 nm; for HI we used 1.0584 and 1.3229 nm. The resulting coefficients are listed in Table IX, and the corresponding values for $\mu(x)$ at various internuclear separations are given in the fourth column of Tables V through VIII for the individual molecules.

One can see from these tables, and graphically from Figs. 2–5, that $\mu_{\text{Padé}}$ [Eq. (6)] agrees with μ_{series} [Eq. (1)] for small x, and with the *ab initio* results μ_{MCSCF} for large internuclear separations. We will discuss the overall accuracy of the present results along with a comparison of previous work in the following section; it is however apparent from these figures that the Padé form is clearly superior to the series expansion for extrapolation, e.g., in order to calculate higher overtone intensities.

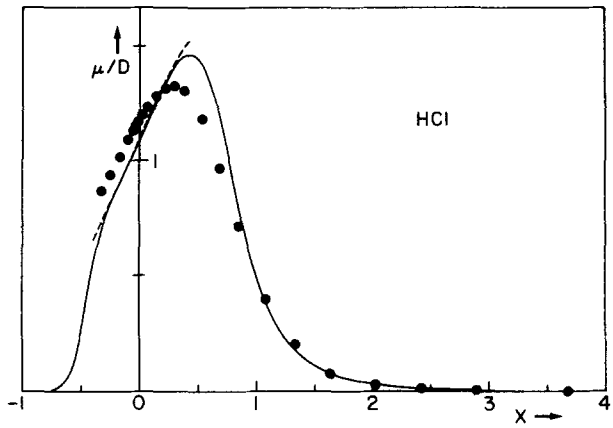

FIG. 3. Dipole moment functions for the ground $X\,^1\Sigma$ state of HCl. The dashed curve is μ_{series}; the solid curve is $U_{\text{Padé}}$; the ● are the *ab initio* values.

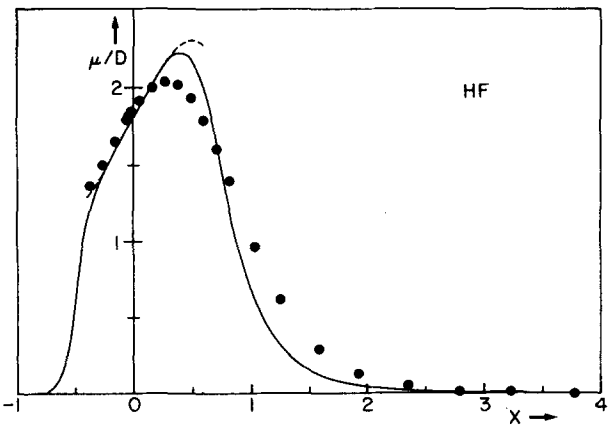

FIG. 2. Dipole moment functions for the ground $X\,^1\Sigma$ state of HF. The dashed curve is μ_{series}; the solid curve is $\mu_{\text{Padé}}$; the ● are the *ab initio* values.

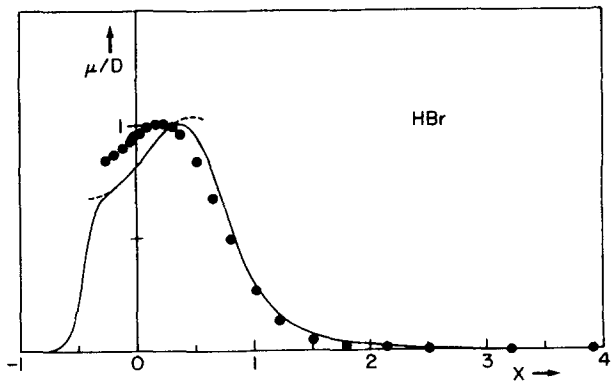

FIG. 4. Dipole moment functions for the ground $X\,^1\Sigma$ state of HBr. The dashed curve is μ_{series}; the solid curve is $\mu_{\text{Padé}}$; the ● are the *ab initio* values.

TABLE X. Comparison of dipole moments (D) for HF computed using various MCSCF type wave functions.

R (10^{-10} m)	This work				
	Lie[a]	Two-term MCSCF	APSG	Five-term MCSCF	Amos[b]
0.917	1.816	1.816	1.865	1.868	1.837
1.588	1.641	1.634[c]	1.693	1.781	1.778
2.117	0.600	0.595[c]	0.617	0.753	0.773
2.646	0.155	0.154[c]	0.157	0.246	0.265
5.292	0.002	0.002[c]	0.002	0.013	0.012
13.000	...	0.0	0.0	0.017	...

[a]Reference 31.
[b]Reference 48.
[c]Interpolated from the results of Table V.

V. DISCUSSION AND COMPARISON WITH PREVIOUS WORK

The first few dipole-moment coefficients for each hydrogen halide in Table III are similar in magnitude and sign to those published in the previous review,[1] with the exception of M_4 for HCl that was incorrectly inferred from molecular beam measurements.[46] We have been able to extend the series expansions for HCl, HBr, and HI based on the recently available experimental data of overtone intensities. In addition, we have in the present study used more accurate matrix elements (correct through a_6 in the potential) than previously. The present agreement in the Herman–Wallis coefficients is also better; because of the nature of these terms (small rotational corrections to the individual line intensities) and the experimental inaccuracies associated with their determination, the overall agreement is considered good.

The dipole coefficients listed in Table III for HCl agree reasonably well with those published by Niay *et al.*[47] for DCl (these dipole moment functions should be the same within the Born–Oppenheimer approximation[48]); most of the minor differences can be attributed to the additional term in our series. For HI, our results are in excellent agreement with the first four coefficients produced by Bernage and Niay,[8] but we disagree about the sign and magnitude of M_4. Although some of the disagreement may again be attributed to an additional term in our expansion, some also results from the use of more accurate matrix elements in the present study. Similar comments apply to HBr for which our results for M_4 and M_5 differ somewhat from those previously published.[7]

The computed dipole moment values for HF, HCl, and HBr are in satisfactory agreement with the results from experiment in the range in which they can be compared. For all three cases they slightly overestimate the experimental values near R_e, and appear to underestimate the values of the maxima in the dipole moment functions. The discrepancy between *ab initio* and experimentally derived values of dipole moment near R_e increases with the number of electrons in the hydrogen halide molecule. For HF we can make comparison for $R<1.0$ nm also with the computed values of Lie[31] and Amos.[49] (More accurate computations[38] are limited to values of R near R_e.) As anticipated in Sec. III above, our results are close to those of Lie[31] but differ markedly at large R from those of Amos.[49] Although the latter results are from a MCSCF computation slightly more extensive than ours as it contains a limited treatment of fluorine intrapair correlation, close inspection reveals that the difference between the two long-range dipole moment functions is due to an inadequacy in the dissociation behavior of Amos's wave function: The correct dissociation of the two-term MCSCF wave functions into neutral atoms is removed by the introduction of the intrapair doubly excited configurations, such as $\pi_x^2 \rightarrow \pi_x^{*2}$, *without* the corresponding quadruply excited configurations, such as $\sigma^2\pi_x^2 \rightarrow \sigma^{*2}\pi_x^{*2}$, that are necessary to describe the correct dissociation of the wave function incorporating the doubly excited configurations. This omission of the quadruply excited configurations leads to residual ionic character of the dissociation products. This conclusion is illustrated in Table X, in which we compare for HF the dipole moments of Amos[49] and Lie[31] at selected internuclear separations with three series of computations performed with our basis set: first, the results of our two-term MCSCF computations reported above; second, MCSCF computations performed using the same five configurations listed by Amos; and third, the antisymmetrized product of strongly orthogonal geminal (APSG) computations in which the four intrapair excitations used by Amos to construct a five-term MCSCF wave function have been used to form four rank-two geminals. Such an APSG wave function implicitly includes the quadruple excitations necessary to retain correct dissociation behavior. Evidently, the differences in the basis sets lead to only small variations in the computed dipole moments, with our two-term MCSCF results agreeing well with those of Lie,[31] and our five-term MCSCF results being close to those of Amos.[49] Furthermore, at large R, the APSG results are close to those from the two-term MCSCF computations, in marked contrast with the five-term MCSCF computation for which incorrect dissociation is demonstrated by *increase* of dipole moment as R increases beyond 0.5 nm; such behavior is of course expected for a wave function giving dissociation products with some ionic character.

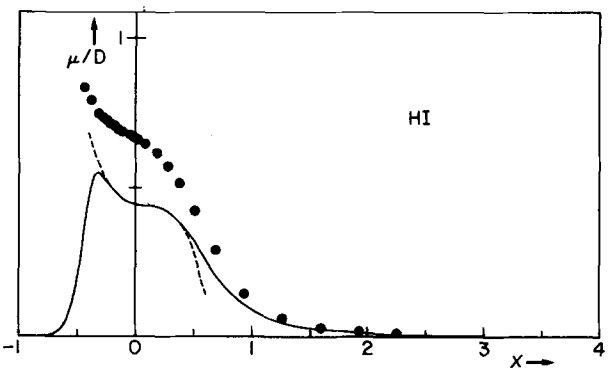

FIG. 5. Dipole moment functions for the ground $X\,^1\Sigma$ state of HI. The dashed curve is μ_{series}; the solid curve is $\mu_{\text{Padé}}$; the ● are the *ab initio* values.

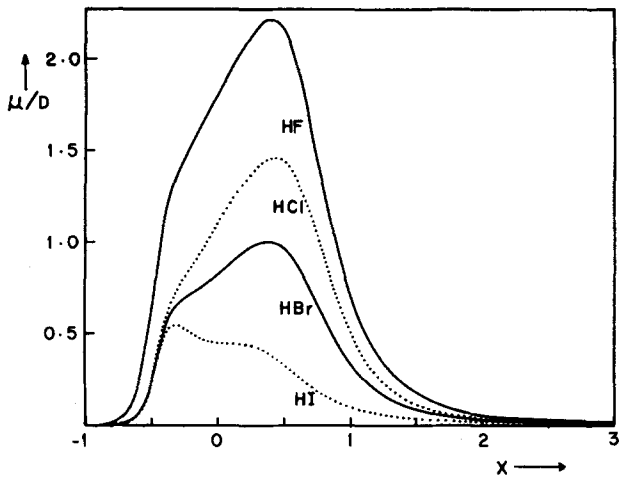

FIG. 6. Comparison of dipole moment functions in Padé approximant form of the four hydrogen halide molecules. —, HF; ···, HCl; —, HBr; ···, HI.

Although the computed dipole moments approach zero less rapidly than expected for $R<R_e$, this region is not important for our present purpose. Much more extensive computations would be necessary to effect significant improvement in this region. As previously noted,[50] the dipole moment function of HI differs qualitatively from that of the other hydrogen halides, as best illustrated in Fig. 6, in which are displayed the four functions each in Padé form. Our analyses from both experimental data and *ab initio* results[11] show this significant difference in shape. Inclusion of relativistic effects seem unlikely to explain this behavior, because relativistic contractions dominate at $R \leq R_e$, relatively increasing the computed dipole moment, whereas expansion occurs at larger R thus decreasing the dipole moment [P. Pyykkö (private communication)]; therefore, inclusion of these effects would not explain the fact that the sign of M_1 is negative for HI but positive for the other hydrogen halides (cf. Table III).

Before concluding this section, we note that the choice of form of the Padé approximant is not unique. In fact, a previous application[51] of this type of function for the dipole moment of HCl employed a ratio of two quadratic functions. Although we have chosen a numerator that approaches zero as R^3 for small R, the true dipole moment function would be expected to conform to this behavior only within a small range near $x=-1$. Our choice affects the function at larger values of x, but the shoulder, or equivalently the point of inflection, that occurs near $x=-0.5$ in all cases in Fig. 6 is dictated by the experimental data and not by the precise form of the numerator utilized in our fitting procedure. Fortunately, the exact shape of the dipole moment function in this region is not crucial for the accurate determination of matrix elements for low-lying vibrational levels. Other choices for the form of the numerator produce no more realistic shapes. In the long-range region ($0.5<x<5$, the Padé function may possibly not be quantitatively accurate, even allowing for sources of error propagating from experimental data or from model deficiencies in the quantum computations. However, the reasonable agreement between computed values and the Padé function values in the region $0.5<x<2.5$ indicates that the Padé function is unlikely to be greatly misleading in this region. Finally, we point out that the Padé form [Eq. (6)] can readily be modified to agree with additional derivatives at $x=0$ if these become available from experimental measurements on the higher overtones.

VI. CONCLUSION

Experimental intensity data for the stable hydrogen halide molecules have been systematically analyzed in order to determine the coefficients of the dipole moment series expansion. This form of the dipole moment function is adequate for representing the lower overtone vibration–rotational line intensities. New *ab initio* quantum computations of the dipole moment function have been carried out over a large range of internuclear separations. At large R they agree well with the theoretical R^{-4} dependence. Information from both of these sources can be combined to produce a semiempirical model of the dipole moment function in the form of a Padé approximant which is constrained to agree with the series expansion near equilibrium, but which incorporates the correct long- and short-range behavior and limits. This form can be used to estimate the transition moments for any bound state, and given the limitations of the experimental data and the corresponding uncertainties of the purely quantum calculations, is probably the best dipole moment function presently available for these molecules.

ACKNOWLEDGMENTS

We are grateful to Drs. C. M. Clayton, P. Pyykkö, and M. Zughul for making results available to us prior to publication, and to Professor D. P. Craig for helpful discussion.

APPENDIX

As mentioned in the text, one can use the Herman–Wallis coefficients in order to determine the relative signs of the rotationless dipole moment matrix elements. Expressions for $C_n(0)$ and $D_n(0)$ for $n=0$ through 4 have been published previously,[29] and the leading terms for $C_5(0)$ and $D_5(0)$ derived in the same way are given here:

$$C_5(0)=2\gamma\Big[\epsilon_0\Big(-\frac{1}{128}a_1^4-\frac{1}{16}a_1^2a_2-\frac{11}{120}a_1a_3-\frac{1}{40}a_2^2-\frac{1}{20}a_4+\frac{3}{16}a_1^3+\frac{9}{20}a_1a_2+\frac{a_3}{5}-\frac{21}{20}a_1^2-\frac{3}{5}a_2+2a_1-\frac{6}{5}\Big)$$
$$+\epsilon_1\Big(-\frac{5}{16}a_1^3-\frac{5}{6}a_1a_2-\frac{5}{12}a_3+\frac{5}{4}a_1^2+\frac{3}{4}a_2-\frac{13}{6}a_1+\frac{5}{4}\Big)+\epsilon_2\Big(-\frac{15}{8}a_1^2-\frac{7}{6}a_2+\frac{5}{2}a_1-\frac{4}{3}\Big)+\epsilon_3\Big(-\frac{7}{2}a_1+\frac{3}{2}\Big)+\epsilon_4(-2)\Big]\,, \tag{A1}$$

$$D_5(0)=\frac{C_5(0)^2}{4}+2\gamma^2\Big[\epsilon_0\Big(\frac{1}{8}a_1^3+\frac{a_1a_2}{3}+\frac{a_3}{6}-\frac{13}{8}a_1^2-a_2+\frac{31}{6}a_1-\frac{9}{2}\Big)+\epsilon_1\Big(-\frac{315}{1024}a_1^5-\frac{215}{128}a_1^3a_2-\frac{93}{64}a_1^2a_3+\frac{17}{32}a_1a_4+\frac{41}{64}a_1a_2^2$$
$$+\frac{37}{24}a_2a_3+\frac{7}{8}a_5-\frac{315}{1024}a_1^4-\frac{255}{128}a_1^2a_2-\frac{143}{64}a_1a_3-\frac{39}{64}a_2^2-\frac{27}{32}a_4-\frac{5}{16}a_1^3-\frac{5}{4}a_1a_2-\frac{11}{12}a_3+\frac{65}{32}a_1^2+\frac{35}{24}a_2-\frac{45}{8}a_1$$
$$+\frac{14}{3}\Big)+\epsilon_2\Big(-\frac{505}{128}a_1^4-\frac{13}{4}a_1^2a_2+\frac{47}{24}a_1a_3+\frac{25}{8}a_2^2+\frac{9}{4}a_4-\frac{255}{64}a_1^3-\frac{117}{16}a_1a_2-\frac{9}{4}a_3-\frac{15}{4}a_1^2-3a_2+\frac{27}{4}a_1-5\Big)$$
$$+\epsilon_3\Big(-\frac{759}{64}a_1^3+\frac{123}{16}a_1a_2+\frac{19}{4}a_3-\frac{819}{64}a_1^2-\frac{81}{16}a_2-\frac{21}{2}a_1+\frac{23}{4}\Big)+\epsilon_4\Big(-\frac{33}{4}a_1^2+11a_2-\frac{27}{2}a_1-8\Big)+\epsilon_5\Big(\frac{25}{4}a_1-\frac{15}{4}\Big)+\epsilon_6(6)\Big], \tag{A2}$$

where

$$\epsilon_i=\frac{\sqrt{15}\gamma^{5/2}M_i}{2\langle 0|\mu|5\rangle}. \tag{A3}$$

Wherever possible, these formula have been checked against, and agree with, the expressions given by Bouanich[5]; however, it should be pointed out that one can not derive the coefficients of ϵ_0 from his results since they were not carried out to sufficiently high order perturbation.

[1]R. H. Tipping and J. F. Ogilvie, J. Mol. Struct. **35**, 1 (1976).
[2]R. H. Tipping, J. Chem. Phys. **59**, 6433 (1973).
[3]R. H. Tipping, J. Chem. Phys. **59**, 6443 (1973).
[4]P. Niay, C. Coquant, and P. Bernage, Can. J. Phys. **57**, 572 (1979).
[5]J. P. Bouanich and C. Brodbeck, J. Quant. Spectrosc. Radiat. Transfer **16**, 153 (1976); J. P. Bouanich, J. Quant. Spectrosc. Radiat. Transfer **16**, 1119 (1976); **17**, 639 (1977); **19**, 381 (1978); **20**, 419 (1978).
[6]M. Zughul (private communication); Bull. Am. Phys. Soc. **25**, 288 (1980), abstract GC3.
[7]P. Bernage and P. Niay, J. Quant. Spectrosc. Radiat. Transfer **18**, 315 (1977).
[8]P. Niay, P. Bernage, C. Coquant, and R. Houdart, Can. J. Phys. **56**, 727 (1978).
[9]R. N. Sileo and T. A. Cool, J. Chem. Phys. **65**, 117 (1976).
[10]R. S. Mulliken and W. C. Ermler, *Diatomic Molecules—Results of ab initio Calculations* (Academic, New York, 1977).
[11]S. R. Ungemach, H. F. Schaeffer, and B. Liu, J. Mol. Spectrosc. **66**, 99 (1977).
[12]J. S. Muenter and W. Klemperer, J. Chem. Phys. **52**, 6033 (1970).
[13]R. J. Lovell and W. F. Herget, J. Opt. Soc. Am. **52**, 1374 (1962).
[14]R. E. Meredith, J. Quant. Spectrosc. Radiat. Transfer **12**, 485 (1972).
[15]R. L. Spellicy, R. E. Meredith, and F. G. Smith, J. Chem. Phys. **57**, 5119 (1972).
[16]G. Rimpel, Z. Naturforsch. Teil A **29**, 588 (1974).
[17]E. W. Kaiser, J. Chem. Phys. **53**, 1686 (1970).
[18]F. G. Smith, J. Quant. Spectrosc. Radiat. Transfer **13**, 717 (1973).
[19]R. A. Toth, R. H. Hunt, and E. K. Plyler, J. Mol. Spectrosc **32**, 74 (1969); **32**, 85 (1969); **35**, 110 (1970).
[20]O. B. Dabbousi, W. L. Meerts, F. H. de Leeuw, and A. Dymanus, Chem. Phys. **2**, 473 (1973).
[21]H. J. Babrov, A. L. Shabott, and B. S. Rao, J. Chem. Phys. **42**, 4124 (1965).
[22]F. A. Van Dijk and A. Dymanus, Chem. Phys. Lett. **5**, 387 (1970).
[23]G. Ameer and W. Benesch, J. Chem. Phys. **37**, 2699 (1962).
[24]C. Meyer, C. Haeusler, and P. Barchewicz, J. Phys. (Paris) **26**, 305 (1965).
[25]J. F. Ogilvie and D. Koo, J. Mol. Spectrosc. **61**, 332 (1976).
[26]C. M. Clayton, Ph.D. thesis, Pennsylvania State University (November, 1977).
[27]P. Niay, P. Bernage, C. Coquant, and A. Fayt, Can. J. Phys. **55**, 1829 (1977).
[28]P. Niay, P. Bernage, and C. Coquant, J. Mol. Spectrosc. **72**, 168 (1978).
[29]R. H. Tipping, J. Mol. Spectrosc. **61**, 272 (1976).
[30]R. H. Tipping and J. F. Ogilvie (to be published).
[31]G. C. Lie, J. Chem. Phys. **60**, 2991 (1974).
[32]F. B. van Duijneveldt, IBM Technical Research Report RJ945, 16437 (December, 1971).
[33]S. Huzinaga, J. Chem. Phys. **42**, 1293 (1965).
[34]S. Huzinaga, *Approximate Atomic Wavefunctions II* (University of Alberta, Edmonton, 1971).
[35]T. H. Dunning, J. Chem. Phys. **66**, 1382 (1977).
[36]T. H. Dunning, Los Alamos Scientific Laboratory Report No. LA-UR-76-2050, (1976).
[37]P. Botschwina and W. Meyer, Chem. Phys. **20**, 43 (1977).
[38]W. Meyer and P. Rosmus, J. Chem. Phys. **63**, 2356 (1975).
[39]R. Albrichs, F. Keil, H. Lischka, W. Kutzelnigg, and V. Staemmler, J. Chem. Phys. **63**, 455 (1975).
[40]V. R. Saunders and M. F. Guest, Proceedings of the SRC Atlas Symposium No. 4, *Quantum Chemistry—the State of the Art* (Chilton, Radnor, PA. 1975), p. 119.
[41]J. Goodisman, J. Chem. Phys. **38**, 2597 (1963).
[42]H. J. Werner and W. Meyer, Mol. Phys. **31**, 855 (1976).
[43]M. B. King and N. M. Queen, J. Chem. Eng. Data **24**, 178 (1979).
[44]S. M. Kirschner, R. J. LeRoy, J. F. Ogilvie, and R. H. Tipping, J. Mol. Spectrosc. **65**, 306 (1977).
[45]F. P. Billinglsey, J. Chem. Phys. **62**, 864 (1975).
[46]E. W. Kaiser, J. Mol. Spectrosc. **77**, 143 (1979).
[47]P. Niay, C. Coquant, P. Bernage, and H. Boquet, J. Mol. Spectrosc. **65**, 388 (1977).
[48]H. Kato, Chem. Phys. Lett. **36**, 256 (1975).
[49]R. D. Amos, Mol. Phys. **35**, 1765 (1978).
[50]R. H. Tipping and A. Forbes, J. Mol. Spectrosc. **39**, 65 (1971).
[51]J. M. Herbelin and G. Emanual, J. Chem. Phys. **60**, 689 (1974).